Optimal Motion Planning for Free-Flying Robots

R. Lampariello*, S. Agrawal**, G. Hirzinger*
*Institute of Robotics and Mechatronics
German Aerospace Center (DLR)
82234 Weßling, Germany
Roberto.Lampariello@dlr.de
**Department of Mechanical Engineering
University of Delaware
Newark, DE 19716
Agrawal@me.udel.edu

***Abstract*— This paper addresses the problem of motion planning for free-flying robots. Full state actuation is considered to allow for large displacements of the spacecraft. Motion planning is formulated as an optimization problem and kinematic as well as dynamic constraints are considered. The chosen optimization criteria are spacecraft actuation and final time. The proposed method allows solutions which do not require any spacecraft actuation for those end goals for which the robot motion is sufficient.**

I. INTRODUCTION

This paper deals with the general problem of motion planning for free-flying robots. Much effort has already been dedicated to such a problem, with the dynamic interaction between the robot motion and the base (spacecraft). The non-integrability of the angular momentum conservation law has given rise to interesting path planning problems and solutions ([1], [2], [3] to mention a few). These problems however deal with a particular case of free-flying robot dynamics, for which it is assumed that no external actions are present. For this case, the robot is often termed free-floating as opposed to free-flying. It is however more generally true that a free-flying robot will be subject to spacecraft control actions, for large displacements, as well as to non-negligible orbital disturbances. The free-floating approximation can only be reasonably assumed in some specific situations, where the robot is engaged in $local\ motions$ and $short\ operations$. Otherwise, the free-floating assumption is not valid. It is perhaps then useful to consider the path planning problem in a more general context.

The first point to note is that in space energy is indeed precious, at least in the form of thruster fuel. The motion planning strategy should then account for this and be in this sense optimal. Since the free-flying operational condition should not necessarily discard the free-floating one - the two should be complementary - the planner should allow solutions to be found for which no base control action is necessary, neglecting orbital disturbances. Furthermore, the final robot-spacecraft configuration should be judiciously chosen, in accordance with the optimality criterion and in relation to the given initial configuration. Of all the possible final robot-spacecraft configurations which result in the desired final state of the robot end-effector in inertial space, the path planning solution should converge to the dynamically optimal one.

The second major point considered here is the fact that the execution of a desired path will necessarily involve some actuator dynamics. A dynamic model of the robot is used together with an optimization routine such that an optimal path can be generated to account for the control bounds. This can ensure that, in the absence of disturbances and modelling simplifications, the desired path is dynamically feasible as well as optimal.

We also point out that a dynamic description of the robot allows the inclusion of models for external actions which are present in Earth orbit. The ETS-VII experiments have in fact shown that these actions (torques) can be significant, at least in Low Earth Orbit [4]. We, however, suggest that these are neglected for the path planning phase and are dealt with by a path tracker which is designed to compensate for them (see [5]).

The modelling of the robot as a fully actuated system also allows to choose between different operational strategies, free-flying (actuation on all spacecraft and robot states), free-floating (actuation on robot states) or attitude controlled (actuation on rotational states of spacecraft and on all robot states). The latter would be necessary, for example, if the attitude of the spacecraft had to be contained within a certain operational window to avoid communication loss with ground. These different strategies can be chosen by simply commanding the desired spacecraft behavior in the desired state variables definition.

The general problem of robot optimal motion planning has been addressed in [6], [7], [8]. These authors address real-time applicability as well as collision avoidance for fixed base robots, with various optimization strategies, including multiple shooting, semi-infinite parameter optimization and polytopic representation of collision constraints. The more specific case of free-flying robots is treated in [9], [10], [11]. The first two, however, only treat the free-floating case while the last addresses the collision avoidance problem in detail.

We present here a first step into the direction of developing a planner for the problem described above. A spatial dynamical model is derived for a free-flying robot with six-degree-of-freedom robot arm and with

rheonomically driven joints. An initial and final robot end-effector state (position and orientation) are defined in Cartesian space. The motion planning is then solved as a single shooting problem, with inequality constraints on the joint kinematics and on the actuator dynamics and equality constraints on the final robot end-effector state. Finally, the motion planning is chosen to be done in joint space, rather than in task space, to avoid the problem of dynamic singularities. This does not allow to formulate a Boundary Value Problem, since the final robot configuration is unknown and should derive from the optimal solution.

II. Modelling and Equations of Motion

Consider the free-flying robot shown in figure 1, composed of rigid bodies connected by revolute joints. Every element of the system is characterised by a local frame of reference $\{O^{\,i},\ \underline{\mathbf{e}}^{\,i}\}$, placed at the joint connecting it with the previous element along the kinematic chain. If $i = 0$, the frame of reference is relative to the base body (satellite), placed in some arbitrary position within it, while if $i = \mathrm{e}$, the frame of reference is relative to the end-effector. The inertial frame is expressed as $\{O^{\,I},\ \underline{\mathbf{e}}^{\,I}\}$.

The quantity $\underline{r}^{\,i}$, shown in figure 1, is the position vector of body i. The position of the $i^{\,th}$ revolute joint, whose rotation vector is $\underline{u}^{\,i}$, is described by the variable $\theta^{\,i}$, which is measured relative to an arbitrary initial reference robot configuration. Vectors $\underline{c}^{\,i}$ and $\underline{d}^{\,i}$ represent the distance from the joint to the centre of mass and to the following joint of body i.

The equations of motion of the system with rheonomically driven joints, first described in [5] for the planar case, will now be briefly described for the spatial case. These can first be written in descriptor form using the Newtonian-Eulerian formulation, as follows:
Kinematics:

$$\dot{\underline{r}}^{\,i} \;=\; \underline{v}^{\,i} \tag{1}$$

$$\dot{\mathbf{A}}^{\,i} := \tilde{\boldsymbol{\omega}}^{\,i}\,\mathbf{A}^{\,i} \tag{2}$$

Dynamics:

$$\frac{d}{dt}\left(m^{\,i}\ \underline{v}^{\,i}\right) \;=\; \underline{f}^{\,i} \;+\; \underline{f}_{\,c}^{\,i}\ , \tag{3}$$

$$\frac{d}{dt}\left(\underline{\underline{I}}^{\,i}\,.\,\underline{\omega}^{\,i}\right) \;=\; \underline{t}^{\,i} \;+\; \underline{t}_{\,c}^{\,i} \tag{4}$$

Constraints:

$$\underline{r}^{\,i+1} \;=\; \underline{r}^{\,i} \;+\; \underline{d}^{\,i}, \tag{5}$$

$$\mathbf{A}^{\,i+1} \;=\; \mathbf{B}^{\,i+1}\,\mathbf{A}^{\,i} \tag{6}$$

where $\underline{r}^{\,i}$ is the absolute position, $\mathbf{A}^{i}$ is the direction cosine matrix, $\underline{v}^{\,i}$ the translational velocity and $\underline{\omega}^{\,i}$ the angular velocity of body i relative to the inertial frame (expressed in inertial coordinates in Eq. (2)). $\mathbf{B}^{\,i}$ is the relative rotation matrix between frames i and $i-1$, function of $\theta^{\,i}$. Furthermore, $m^{\,i}$ is the mass, $\underline{\underline{I}}^{\,i}$ the inertia tensor referred to the centre of mass, $\underline{f}^{\,i}$ and $\underline{t}^{\,i}$ are the sums of the external forces and torques and $\underline{f}_{\,c}^{\,i}$ and $\underline{t}_{\,c}^{\,i}$ are the sums of the constraint forces and torques (arising from the revolute joints) on the $i^{\,th}$ body.

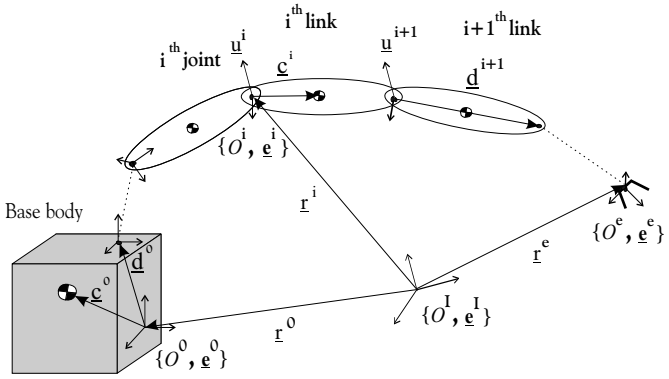

Fig. 1. Reference frames and geometrical quantities of the free-flying robot

After choosing a suitable frame of reference in which to express the vector quantities and a suitable parameterisation of the angular position, as for example Euler angles $\boldsymbol{\phi}^{\,i}$, the equations can be written in matrix form. Choosing the inertial frame $\{O^{\,I},\ \underline{\mathbf{e}}^{\,I}\}$, the kinematic and dynamic equations become:

$$\dot{\mathbf{x}}_{\,I} \;=\; \mathbf{X}(\mathbf{x}_{\,I})\,\mathbf{x}_{\,II} \tag{7}$$

$$\mathbf{J}\,\dot{\mathbf{x}}_{\,II} \;=\; \mathbf{Q} \;+\; \boldsymbol{\Lambda} \;=\; \mathbf{Q} \;+\; \boldsymbol{\tau} \;+\; \boldsymbol{\tau}_{\,c} \tag{8}$$

where

$$\mathbf{x}_{\,I} \;=\; \begin{bmatrix} [\mathbf{r}^{\,i}] \\ [\boldsymbol{\phi}^{\,i}] \end{bmatrix} \qquad \mathbf{x}_{\,II} \;=\; \begin{bmatrix} [\mathbf{v}^{\,i}] \\ [\boldsymbol{\omega}^{\,i}] \end{bmatrix} \tag{9}$$

are vector arrays related by the matrix $\mathbf{X}$, which in turn can be determined by the standard formulation of the Euler angles parameterisation (see for example [12], p.83) and

$$\mathbf{J} = \begin{bmatrix} \mathbf{m} & \mathbf{0} \\ \mathbf{0} & \mathbf{I} \end{bmatrix} \qquad \mathbf{Q} = \begin{bmatrix} \mathbf{0} \\ -\,[\tilde{\boldsymbol{\omega}}^{\,i}\,\mathbf{I}^{\,i}\,\boldsymbol{\omega}^{\,i}] \end{bmatrix} \qquad \boldsymbol{\tau} = \begin{bmatrix} [\mathbf{f}^{\,i}] \\ [\mathbf{t}^{\,i}] \end{bmatrix}. \tag{10}$$

Furthermore, $\mathbf{m} = \mathrm{diag}(\,m^{\,i}\,\mathbf{E}_{\,3}\,)$, where $\mathbf{E}_{\,3}$ is a three dimensional identity matrix, and $\mathbf{I} = \mathrm{diag}(\,\mathbf{I}^{\,i}\,)$.

The differential algebraic equations (7) - (8) with (5) - (6) can then be transformed into a set of ordinary differential equations. The Cartesian position variables of the system defined in Eq. (9) are replaced by the independent position state space variables which can be chosen to be

$$\mathbf{y}_{\,I} \;=\; [\,\mathbf{r}^{\,0},\,\boldsymbol{\phi}^{\,0},\,\boldsymbol{\theta}\,]^{\,T} \quad \mathbf{y}_{\,II} \;=\; [\,\mathbf{v}^{\,0},\,\boldsymbol{\omega}^{\,0},\,\dot{\boldsymbol{\theta}}\,]^{\,T} \tag{11}$$

where $\boldsymbol{\theta} = [\theta^{\,i}]$. The relationship between the variables $\mathbf{x}_{\,II}$ and $\mathbf{y}_{\,II}$ can be expressed as

$$\mathbf{x}_{\,II} \;=\; \boldsymbol{\psi}\,\mathbf{y}_{\,II} \;+\; \hat{\boldsymbol{\psi}}\,\mathbf{z}_{\,II} \tag{12}$$

where $\boldsymbol{\psi}$ is termed the modal matrix. Furthermore, $\mathbf{z}_{\,II}$ includes all the locked and kinematically (or rheonomically) driven velocity state variables of the system (for further details refer to [12]).

Eq. (12) can then be differentiated in time and substituted into Eq. (8) to obtain:

$$\dot{\mathbf{y}}_{\,I} \;=\; \bar{\mathbf{X}}(\mathbf{y}_{\,I})\,\mathbf{y}_{\,II} \tag{13}$$

$$\bar{\mathbf{J}}\,\dot{\mathbf{y}}_{\,II} \;=\; \bar{\mathbf{Q}} \;+\; \bar{\boldsymbol{\tau}}. \tag{14}$$

Note that the resultant equations are now free of the unknown constraint force vector $\boldsymbol{\tau}_{\,c}$, which results from the application of d'Alembert's principle.

A. Rheonomic joints

Noting then that Eq. (12), with rheonomically driven joints, is written as:

$$\mathbf{x}_{\,II} \;=\; \bar{\boldsymbol{\psi}}\,\bar{\mathbf{y}}_{\,II} \;+\; \hat{\bar{\boldsymbol{\psi}}}\,\bar{\mathbf{z}}_{\,II} \;+\; \hat{\bar{\boldsymbol{\psi}}}_{\,l}\,\bar{\mathbf{z}}_{\,II\,l}, \tag{15}$$

where

$$\bar{\mathbf{y}}_{\,II} \;=\; [\,\mathbf{v}^0,\,\boldsymbol{\omega}^0\,]^{\,T}, \quad \bar{\mathbf{z}}_{\,II} = \dot{\boldsymbol{\theta}}, \tag{16}$$

and $\bar{\mathbf{z}}_{\,II\,l}$ now contains only the locked velocity state variables, it follows, using the same procedure above, that the equations of motion become:

$$\dot{\bar{\mathbf{y}}}_{I} \;=\; \bar{\mathbf{X}}^{\,0}(\bar{\mathbf{y}}_{\,I})\,\bar{\mathbf{y}}_{\,II} \tag{17}$$

$$\bar{\mathbf{J}}^{\,0}\,\dot{\bar{\mathbf{y}}}_{II} \;=\; \bar{\mathbf{Q}}^{\,0} \;+\; \bar{\boldsymbol{\tau}}^{\,0} \;+\; \Upsilon. \tag{18}$$

In Eqs. (18) - (18) the superscript 0 relates to the case with rheonomic joints. Also, in the equation

$$\Upsilon = \boldsymbol{\psi}^T\,\mathbf{J}\;\hat{\bar{\boldsymbol{\psi}}}\;\ddot{\boldsymbol{\theta}}^{\,0}, \tag{19}$$

where now $\ddot{\boldsymbol{\theta}}^{\,0}$ is a prescribed function of time.

Note that the order of the equations of motion (18) is now only six, equal to the degrees of freedom of the base body.

B. Modelling summary

From the above derivation it follows that:

- the fully-actuated system is represented by Eqs. (14) - (14) - note that actuation on the spacecraft and robot is expressed by vector $\bar{\boldsymbol{\tau}}$;
- the fully-actuated system with rheonomically driven joints is represented by Eqs. (18) - (18) - note that actuation on the robot does not appear, as its motion is described by the prescribed time function $\ddot{\boldsymbol{\theta}}^{\,0}$. Actuation on the spacecraft is expressed by vector $\bar{\boldsymbol{\tau}}^{\,0}$;
- the free-floating system is described by Eqs. (14) - (14) or by Eqs. (18) - (18) for $\bar{\boldsymbol{\tau}}^{\,0} = 0$.

III. Trajectory planning

The path planning problem is generally defined here as the point-to-point problem, i.e. that of determining the time history of the robot joints and spacecraft state (position and orientation) in order to move the end-effector of the robot from a given initial to a given final state in inertial space. As we are considering the trajectory planning problem, the equivalent time history for the actuation variables will also be determined.

Using the notation in figure 1, the initial and final end-effector position and orientation are defined as:

$$\underline{r}^{\,e}(t_{\,0}) \;=\; \underline{r}^{\,e}_{\,0} \qquad \underline{\phi}^{\,e}(t_{\,0}) \;=\; \underline{\phi}^{\,e}_{\,0} \tag{20}$$

$$\underline{r}^{\,e}(t_{\,f}) \;=\; \underline{r}^{\,e}_{\,\mathrm{des}} \qquad \underline{\phi}^{\,e}(t_{\,f}) \;=\; \underline{\phi}^{\,e}_{\,\mathrm{des}}\;, \tag{21}$$

where $t_{\,0}$ and $t_{\,f}$ are the initial and final time of the maneuver and $\underline{\phi}^{\,e}$ is a set of Euler angles to represent the orientation of the frame of reference $\{O^{\,e}, \underline{\mathbf{e}}^{\,e}\}$

Furthermore, the path planning solution has to satisfy kinematic and dynamic constraints. The former can be expressed as

$$\theta^{\,i}_{\min} \le \theta^{\,i} \le \theta^{\,i}_{\max}\,,\;\; 1 \le i \le n\,, \tag{22}$$

where n is the number of joints of the robot (taken to be six).

The dynamic constraints are simply

$$\bar{\tau}^{\,0\,i}_{\min} \;\le\; \bar{\tau}^{\,0\,i} \le \bar{\tau}^{\,0\,i}_{\max}\,,\;\; 1 \le i \le 6\,, \tag{23}$$

$$\bar{\tau}^{\,i}_{\min} \;\le\; \bar{\tau}^{\,i} \;\le \bar{\tau}^{\,i}_{\max}\,,\;\; 6 < i \le n+6\,, \tag{24}$$

where $\bar{\tau}^{\,i}$ is generally the actuation force for the state variable i and superscript 0 relates to the base body. Note that we are considering the case of full actuation, meaning that the states of the robot are taken to be the six degrees of freedom of the spacecraft ($1 \le i \le 6$) and the n degrees of freedom of the robot ($6 < i \le 6+n$).

As we anticipated in the introduction, the path planning problem is taken as an optimization problem. The $6+n$ states of the robot-spacecraft system are parameterised in time while Eqs. (21) - (21) and (22) - (24) will be taken as equality and inequality constraints respectively. Regarding the cost function, we have initially chosen to optimize for the base actuation in order to minimise for the thruster fuel consumption. We have chosen to optimize for both translational and rotational spacecraft actuation as an example. The cost function Γ can then be expressed mathematically as

$$\Gamma \;=\; \sum_{i=1}^{6} \int_0^{t_{\,f}} \parallel \bar{\tau}^{\,0\,i}(t) \parallel \; dt\,, \tag{25}$$

where Γ can be considered as the impulse, if the torques are assumed to be computed as the product of a force by a unit moment arm. Then the impulse can be related to an energy content because it is equal to the product of the necessary fuel mass times its specific impulse (which is a given constant).

A. Constraint equations

The left hand sides of the equality constraints (21) - (21) are simply expressed as

$$\underline{r}^{\,e} = \underline{r}^{\,0} + \sum_{i=0}^{n} \underline{d}^{\,i} \quad (26)$$

$$\mathbf{A}(\boldsymbol{\phi}^{\,e}) = \mathbf{A}(\boldsymbol{\phi}^{\,0})\,\mathbf{A}(\boldsymbol{\theta}) \quad (27)$$

where $\mathbf{A}$ is a rotation matrix, function of a set of rotation parameters $\boldsymbol{\phi}$ or of joint angles $\boldsymbol{\theta}$.

For inequality constraints (22) - (24), the inverse dynamics problem has to be solved. Given a time history of the $6+n$ state variables $\mathbf{y}_{\,I} = [\,\mathbf{r}^{\,0}\ \boldsymbol{\phi}^{\,0}\ \boldsymbol{\theta}\,]^{\,T}$ and their first and second derivatives $\dot{\mathbf{y}}_{\,I} = [\,\mathbf{v}^{\,0}\ \boldsymbol{\omega}^{\,0}\ \dot{\boldsymbol{\theta}}\,]^{\,T}$ and $\ddot{\mathbf{y}}_{\,I} = [\,\dot{\mathbf{v}}^{\,0}\ \dot{\boldsymbol{\omega}}^{\,0}\ \ddot{\boldsymbol{\theta}}\,]^{\,T}$, then the vector of actuator actions $\bar{\boldsymbol{\tau}}$ is given by Eq. (14).

B. Use of the free-floating solution

The equations defined in the previous section are conceptually complete for the solution of the path planning problem we are wanting to solve. However, in order to improve the quality of the optimal solutions and the efficiency of the optimizing routine a further step is introduced. We first want to distinguish between maneuvers in what we define the $local\ workspace$ - the workspace of the robot with no spacecraft actuation - and those in the $global\ workspace$ - ideally all reachable free space. The distinction is useful here because the first kind of maneuver does not $require$ any spacecraft actuation and the optimal solution in the sense we have defined should be exactly this one. This can be called the $free\text{-}floating\ solution$. The motion of the base for these solutions is complex or in any case would require a polynomial of high degree in order for it to be suitably approximated. A high degree polynomial means a high number of optimization parameters and a longer running time for the optimization algorithm.

An alternative approach is to solve for the free-floating motion for a given time evolution of the joints and add this to a parametric function of the spacecraft states, such that the latter can be simply set to zero if free-floating solutions are sought. Although one might argue that the overall running time is comparable to that of the previous approach, we have chosen to go this way. A free-floating solution can in this way be described exactly.

Therefore, equations of motion (18) - (18) for the free-flying robot with rheonomically driven joints are used. The integration of Eq. (18) supplies the solution $\bar{\mathbf{y}}_{\,II}^{\,ff} = [\mathbf{v}^{\,ff}\ \boldsymbol{\omega}^{\,ff}\,]^{\,T}(t)$, the free-floating solution. Note that this solution depends on the joint motion variables, which are parameterised in time. The free-floating solution can then be added to a time parameterised term to finally satisfy the equality constraints (21) - (21) (see section IV). The inequality constraints (24) - (24) can then be satisfied by use of Eq. (14).

IV. Trajectory planning solver

The optimization problem is then:

$$\min_{\mathbf{p}}\ \Gamma \quad (28)$$

where $\mathbf{p}$ is the set of parameters appearing in the states parametric functions defined below. The cost function is given by Eq. (25) and Eqs. (21) - (21) and (22) - (24) are the equality and inequality constraints respectively.

Furthermore, the parameterisation of the state variables is as follows:

$$\mathbf{r}^{\,0}(t) = \mathbf{r}^{\,ff}(t) + f_t^{\,5}(t;\mathbf{p}) \quad (29)$$

$$\mathbf{v}^{\,0}(t) = \mathbf{v}^{\,ff}(t) + f_t^{\,4}(t;\mathbf{p}) \quad (30)$$

$$\dot{\mathbf{v}}^{\,0}(t) = \dot{\mathbf{v}}^{\,ff}(t) + f_t^{\,3}(t;\mathbf{p}) \quad (31)$$

$$\mathbf{A}(\boldsymbol{\phi}^{\,0})(t) = \mathbf{A}(\boldsymbol{\phi}^{\,0})(0) \int_0^t \tilde{\boldsymbol{\omega}}^{\,0}\,\mathbf{A}(\boldsymbol{\phi}^{\,0})\,d\bar{t} \quad (32)$$

$$\boldsymbol{\omega}^{\,0}(t) = \boldsymbol{\omega}^{\,ff}(t) + f_r^{\,4}(t;\mathbf{p}) \quad (33)$$

$$\dot{\boldsymbol{\omega}}^{\,0}(t) = \dot{\boldsymbol{\omega}}^{\,ff}(t) + f_r^{\,3}(t;\mathbf{p}) \quad (34)$$

$$\theta^{\,i}(t) = f_j^{\,5}(t;\mathbf{p}) \quad 1 \le i \le n \quad (35)$$

$$\dot{\theta}^{\,i}(t) = f_j^{\,4}(t;\mathbf{p}) \quad 1 \le i \le n \quad (36)$$

$$\ddot{\theta}^{\,i}(t) = f_j^{\,3}(t;\mathbf{p}) \quad 1 \le i \le n \quad (37)$$

where generally function $f^{\,n}$ is a polynomial function of degree n and given a polynomial function of degree i, e.g. $f_j^{\,5}$, then the following polynomial functions of degree $i-1, i-2$ are the successive derivatives of the first. These functions have been parameterised with a polynomial of degree 5 in order to set the further desired conditions that:

- velocity and acceleration of parameterised variables are at initial and final time zero;
- the initial position is given by the definition of the initial conditions of the robot-spacecraft configuration.

It follows that parameter vector $\mathbf{p}$ is composed of the following quantities:

$$\mathbf{p} = [\,\theta^{\,1}\ \theta^{\,2}\ \theta^{\,3}\ \theta^{\,4}\ \theta^{\,5}\ \theta^{\,6}\ {r^{\,0\,1}}_b\ {r^{\,0\,2}}_b\ {r^{\,0\,3}}_b\ {\phi^{\,0\,1}}_b\ {\phi^{\,0\,2}}_b\ {\phi^{\,0\,3}}_b\,]^{\,T}\ (t_{\,f}), \quad (38)$$

where ${r^{\,0\,i}}_b$ are the components of the second term on the right hand side of Eq. (30) and ${\phi^{\,0\,i}}_b$ are the equivalent for the rotational motion. The latter are such that the integral of the angular velocity $\boldsymbol{\omega}^{\,0}$ (Eq. (33)) satisfies the orientation constraint on the end-effector. Furthermore, each of the first terms on the right hand side of Eqs. (30) - (35) is taken from the solution (integration) of Eq. (18), which is in turn obtained with the aid of Eqs. (36) - (37) . Eqs. (30) - (37) are then used with Eq. (14) to compute vector $\bar{\boldsymbol{\tau}}$.

Note that the chosen polynomial parameterisation for the state variables allows only one free parameter for each position variable. This is the minimum number of

parameters possible and a broader range of functions could be used for the optimization problem by choosing higher degree polynomials or B-splines, for possibly better optimal solutions, but at the clear expense of computation time. As a first approach the simplest function representation was chosen here.

Furthermore, due to the boundedness of function θ^{i}(t) between $\theta^{i}\,(t_{0})$ and $\theta^{i}\,(t_{f})$, the kinematic inequality constraints only need to be checked at $t = t_{f}$.

The optimization method used for the resolution of the above problem is Sequential Quadratic Programming (SQP).

V. Results

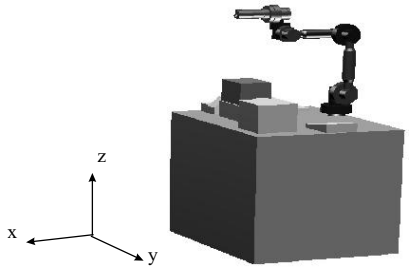

Fig. 2. Model example of free-flying robot. Initial configuration is shown.

Two paths are considered for the description of the proposed method: a path in the local workspace and a path in the global workspace. Consider the free-flying robot shown in figure 2. The inertial parameters of the robot where chosen to be those of the ETS-VII satellite. The initial state of the end-effector corresponding to the shown configuration of the robot is:

$$\underline{r}\,{}^{e}_{0} = [\,0.10\ -0.83\ 4.49\,]^{T}\quad \underline{\phi}\,{}^{e}_{0} = [\,0.0\ 0.0\ 0.0\,]^{T}.$$

For the first path, the final desired state of the end-effector was chosen to be

$$\underline{r}\,{}^{e}_{\mathrm{des}} = [\,0.40\ 0.0\ 3.8\,]^{T}\quad \underline{\phi}\,{}^{e}_{\mathrm{des}} = [\,-0.5\ 0.5\ 0.0\,]^{T}.$$

The initial guess was taken to be
$\mathbf{p}_{0} = [\,0.1\ 0.1\ 0.1\ 0.1\ 0.1\ 0.1\ 0.0001\,...\ 0.0001\,]^{T}$.
The solution was hence found to be
$\mathbf{p} = [\,0.85\ 0.62\ -0.20\ 0.40\ -0.94\ 0.12\ 0.0\,...\ 0.0\,]^{T}$.
The cost function for this example was 8 e-3 kg m/s, indicating that no base actuation is present (this is also clear from the zero values of the last six parameters). The path is shown in Fig. 3. The computation time was about 130 seconds on a standard Sgi machine. For the second maneuver, the final desired state of the end-effector was chosen to be

$$\underline{r}\,{}^{e}_{\mathrm{des}} = [\,6.0\ -0.83\ 7.00\,]^{T}\quad \underline{\phi}\,{}^{e}_{\mathrm{des}} = [\,0.0\ 0.0\ 0.0\,]^{T}.$$

The initial guess was taken to be the same as for the previous case. The solution was hence found to be

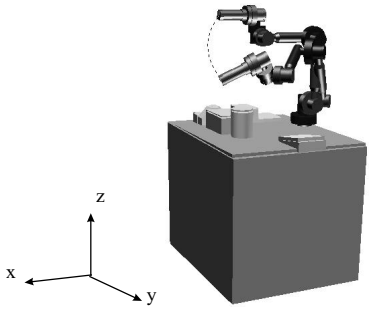

Fig. 3. Maneuver in local workspace - free-floating solution. Initial and final configurations are shown.

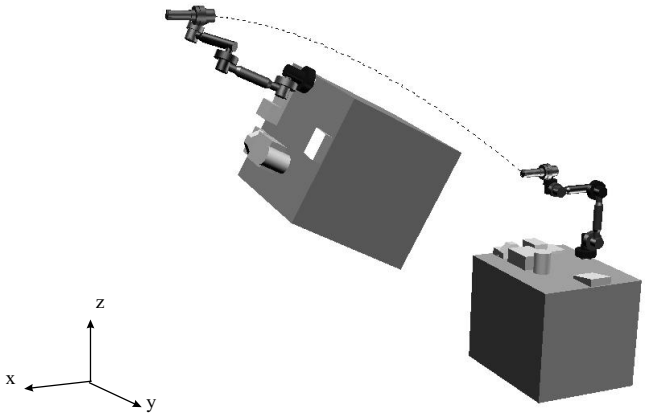

Fig. 4. Maneuver in global workspace. Initial and final configurations are shown.

$\mathbf{p} = [\,-1.35\ 0.3\ -0.94\ -0.88\ 0.45\ 1.37\ 1.97\ 0.42\ 3.94\ 0.03\ 1.09\ -0.07\,]^{T}$.

The cost function for this case was 4460 kg m/s, of which 1815 kg m/s from the translational forces. The computation time was about 165 seconds. The path is shown in Fig. 4. Kinematic constraints (22) were applied as

$$\theta^{i}_{\min} = -1.5,\quad \theta^{i}_{\max} = +1.5\,,\ 1 \le i \le n\,.$$

The spacecraft actuator's effort is shown in Fig. 5, for the spacecraft actuation torque $\tau^{0\,4}$. Note that the final time t_{f} is 50.0 seconds. The chosen parameterisation however does not allow to lower the control bounds below the found solution since the parameterisation function is only dependent on the final robot-spacecraft position. However, to avoid saturation of the actuators within the context of trajectory planning, a variable execution time is sufficient. The last maneuver is then repeated with bounds on the base body actuation forces, taken to be

$$\tau^{0\,i}_{\min} = -20.0,\quad \tau^{0\,i}_{\max} = +20.0\,,\ 1 \le i \le 6\,.$$

The results, also given in Fig. 5, are clearly showing the optimal use of the actuators to minimise the final time for the given dynamical limits of the robotic system. The

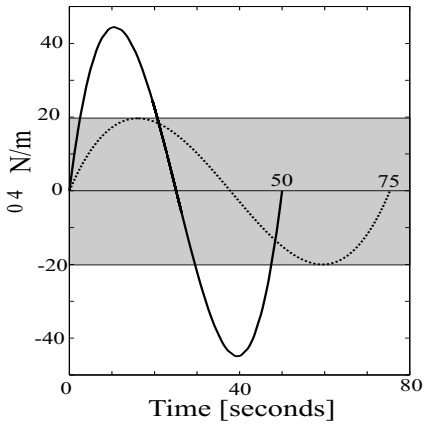

Fig. 5. Spacecraft actuation torque τ^{04} for unbound (continuos line) and bounded solution (dotted line)

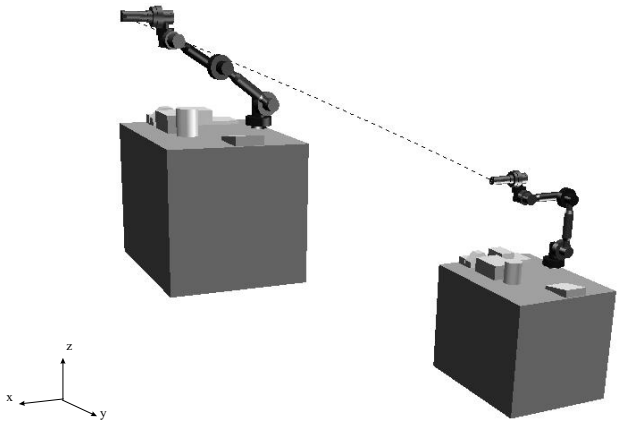

Fig. 6. Maneuver in global workspace - attitude controlled spacecraft for zero angular motion. Initial and final configurations are shown.

final time t_f is now 75.37 seconds. Furthermore, the cost function has been defined as $\Gamma = t_f$, as opposed to the conflicting function defined in Eq. (25).

A. Maneuvers for attitude controlled operational strategy

The second maneuver, shown in Fig. 4, is repeated for the attitude controlled case. This is achieved by simply fixing the desired rotational states of the base to their initial values and the angular velocity and acceleration to zero. The resulting maneuver is shown in Fig. 6. Note that the solution in this case is

$\mathbf{p} = [\,1.00\ \ 1.50\ \ -1.42\ \ -0.08\ \ -1.00\ \ 0.00\ \ 5.46\ \ -1.42\ \ 3.30\ \ 0.00\ \ 0.00\ \ 0.00\,]^T$

and the cost function is 5033 kg m/s, of which 2108 kg m/s from the translational forces. Comparing this result with that of the maneuver shown in Fig. 4, we find that the cost is in this case higher, due to the constraint imposed on the base motion.

B. Orbital disturbances

These could be included in the model to aid the optimal solution. However their effect leads to a monotonic acceleration of the system. Although this could still be of aid for part of the maneuver, we believe that they should be dealt with by the spacecraft control only, gaining in planning simplicity, and because the gain in including them in the dynamic model would be minimal. Only for very slow motions would their effect be of real relevance.

VI. CONCLUSION

An optimization method has been applied to the motion planning problem of free-flying robots. Solutions have been found for local and global motions, where for the latter the unnecessary spacecraft actuation has been shown to be efficiently avoided. Both kinematic and dynamic constraints have been satisfied allowing for minimum spacecraft actuation or minimum time of execution. The times of computation have also been shown to be promisingly short. Further work will address collision avoidance and the development of an initial guess criterion for optimization robustness.

VII. REFERENCES

[1] Y. Nakamura, R. Mukherjee: "Nonholonomic Path Planning of Space Robots via a Bi-Directional Approach", *Proc. of IEEE Int. Conf. on Robotics and Automation (ICRA)*, Cincinnati, OH, May 1990.

[2] Mukherjee, R., Zurowski, M.: "Reorientation of a structure in space using a three-link rigid manipulator", *Journal of Guidance, Control and Dynamics*, Vol.17, No.4, July-August 1994.

[3] Y. Nakamura, T. Suzuki: "Planning Spiral Motions of Nonholonomic Free-Flying Space Robots", *J. of Spacecraft and Rockets*, Vol.34, No.1, Jan.-Feb. 1997.

[4] K. Landzettel, B. Brunner, G. Hirzinger, R. Lampariello, G. Schreiber, B.-M. Steinmetz: "A Unified Groud Control and Programming Methodology for Space Robotics Applications - Demonstrations on ETS-VII", *International Symposium on Robotics (ISR 2000)*, Montreal, Canada, May 2000.

[5] R. Lampariello, G. Hirzinger: "Free-flying Robots - Inertial Parameter Identification and Control Strategies", *ESA Workshop on Advanced Space Technologies for Robotics and Automation*, Estec, Noordwijk, The Netherland, December 2000.

[6] M. C. Steinbach, H.G. Bock, G.V. Kostin, R.W. Longman: Mathematical Optimisation in Robotics: Towards Automated High Speed Motion Planning, *Surveys Math. Indust.* 7(4), 303-340, 1998.

[7] N. Faiz, S. K. Agrawal: "Trajectory Planning of Robots with Dynamics and Inequalities", *Proc. of the IEEE Int. Conf. on Robotics and Automation (ICRA)*, San Francisco, CA, April 2000.

[8] M. Schlemmer, G. Gruebel: ”Real-Time Collision Free Trajectory Optimisation of Robot Manipulators via Semi-Infinite Parameter Optimisation”, *International Journal of Robotics Research*, vol. 17, no.9, September 1998, pp.1013-1021.

[9] V.H. Schulz: ”Reduced SQP Methods for Large-Scale Optimal Control Problems in DAE with Application to Path Planning Problems for Satellite Mounted Robots”, Ph.D. thesis at the University of Heidelberg, 1996.

[10] S. Dubowsky, M. Torres: *Minimizing Attitude Control Fuel in Space Manipulator Systems*, Proc. of the Int. Symp. on Artificial Intelligence: Robotics and Automation in Space, Japan, Nov. 1990.

[11] O. Brock, L.E. Kavraki: *Towards Real-time Motion Planning in High-dimensional Space*, Proc. of the Int. Symp. on Robotics and Automation 2000.

[12] Roberson, E.R.; Schwertassek, R.: *Dynamics of Multibody Systems*, Springer-Verlag, 1988.